Dalton Transactions

Accepted Manuscript

This article can be cited before page numbers have been issued, to do this please use: E. Boccalon, M. Nocchetti, M. Pica, A. Romani and M. Casciola, *Dalton Trans.*, 2017, DOI: 10.1039/C7DT03957C.

ROYAL SOCIETY OF CHEMISTRY

rsc.li/dalton

View Article Online
DOI: 10.1039/C7DT03957C

LAYERED DOUBLE HYDROXIDE AND ZIRCONIUM PHOSPHATE AS ION EXCHANGERS FOR THE REMOVAL OF 'BLACK CRUSTS' FROM THE SURFACE OF ANCIENT MONUMENTS

E. Boccalon[a], M. Nocchetti[b*], M. Pica[b], A. Romani[a], M. Casciola[a]

[a]Dipartimento di Chimica Biologia e Biotecnologie, University of Perugia, Via Elce di Sotto 8, 06123 Perugia, Italy
[b]Dipartimento di Scienze Farmaceutiche, University of Perugia, Via del Liceo 1, 06123, Perugia, Italy.
*Corresponding author: morena.nocchetti@unipg.it

Abstract

The chloride form of MgAl layered double hydroxide (hereafter MgAlCl) as anion exchanger and the semisodic form of α-zirconium phosphate (hereafter ZrPNaH) as cation exchanger are proposed as new cleaning agents for the gypsum removal from ancient monuments. The ability of these exchangers to capture the calcium and sulphate ions of the gypsum powder was first investigated separately and then as coupled system. MgAlCl/gypsum, ZrPNaH/gypsum and MgAlCl/ZrPNaH/gypsum mixtures were characterized by X-ray powder diffraction (XRD), scanning electron microscopy (FE-SEM) and dispersive X-ray spectroscopy (EDX). ZrPNaH in the form of wet paste exhibited a rapid uptake of calcium from gypsum powder via Na^+ and H^+/Ca^{2+} cation exchange. Gypsum powder was also successfully dissolved by a wet paste of MgAlCl by exploiting the Cl^-/SO_4^{2-} anion exchange reaction. However, the dehydration of the paste favoured the reprecipitation of a secondary gypsum that was characterized by lower crystallinity and smaller particle size than the pristine gypsum. The combination of wet MgAlCl and ZrPNaH showed a synergic effect in the gypsum dissolution and partially prevented the gypsum reprecipitation in the dry paste. Finally, a preliminary test of removal of gypsum crust grown on a sandstone sample was performed.

Introduction

The exposure of monuments to the action of atmospheric agents (wind, rain) and pollution leads to important changes in their structure (both physical and chemical) that threaten their conservation. One of these alterations consists in the superficial dissolution of the calcareous matrix of carbonate building stones, like marble or travertine. The surface deterioration is the consequence of the

View Article Online
DOI: 10.1039/C7DT03957C

reaction between limestone and the sulphuric acid present in acidic rains which leads to the conversion of calcite into gypsum, according to the following reaction:

$$CaCO_3 + H_2SO_4 + H_2O \rightarrow CaSO_4 \cdot 2H_2O + CO_2$$

This conversion can be catalysed by iron oxides, hydroxides and organic components that are diffused in the atmosphere due to environmental pollution.[1] Surfaces directly exposed to atmospheric agents are subjected to leaching and the gypsum crystals are easily dissolved and taken away; differently, the sheltered areas promote the development of a crust with a thickness that can increase with time ranging from 60 to 400 μm, completely obscuring and modifying the real characteristic of the stone.[2] The new gypsum layer gradually absorbs pollutants and smog particles, which convert the white colour of the substrate in a crust of dark-grey tonality. Once considered a protective layer, the 'black crusts' are instead a dangerous patina which contributes to the damage of the monuments; gypsum, in fact, exhibits specific volume, porosity and heat capacity that are different from those of marble and all these properties result in a mechanical stress and alteration of the structure so deep that it can produce expansions, fractures and, eventually, detachments.[3] The treatments used so far for the cleaning of the 'black crusts' are mechanical[4-6], biological[7] and chemical. In light of the topic of this paper, only the chemical methods are described. They consist in applying reagents, like ammonium bicarbonate or EDTA, mixed together with cellulose or other medium to create a poultice that is left to dwell for 12-24 hours in contact with the substrate.[8] Once applied, the 'cleaning pack' is immediately covered with a plastic film to prevent the poultice from drying out. The main task of ammonium bicarbonate is to reconvert calcium sulphate in calcium carbonate, whereas the chelating effect of EDTA is used for the complexation of calcium ions and the consequent weakening and dissolution of the encrustation that is then removed by the use of brushes. This kind of treatment needs, in order to reach satisfactory results, long contact times and multiple application, as well as an adequate neutralisation or deionised water rinsing to eliminate potentially harmful residues.

The cleaning packs are easy to be manipulated by operators; they do not require considerable experience, skills or expensive equipment and can be used under all weather conditions without frosting risks. Their costs are minimal and are often selected where more control and sensitivity is required, as in the cleaning of sculptures or decorative masonry details. Besides the slowness of the process, the main drawbacks of the cleaning packs are the risk of reactants migration through the substrate and the need to maintain the poultice always hydrated upon the completion of the procedure. The widespread diffusion of the 'chemical poultices' is mainly related to the absence of any form of abrasion or excessive amounts of water; however, they are not always chemically safe: improper use of EDTA, for example, can affect intact stone surfaces, sequestrating calcium ions

View Article Online
DOI: 10.1039/C7DT03957C

from calcite instead of gypsum.[8] The need to combine efficiency and rapidity in the cleaning treatments, in order to reduce, at the same time, costs and environmental impact, addressed the research both towards the improvement of the traditional techniques and towards the development of more efficient cleaning systems based on new materials. As a matter of fact, the use of solids having ion exchange properties could be an evaluable and alternative strategy in the cleaning of ancient monument surfaces. Among the ion exchangers layered double hydroxides (LDH) and α-zirconium phosphate (ZrP) represent complementary and efficient materials due to their high ion exchange capacity (IEC 4 and 6.5 meq/g for MgAl LDH and ZrP, respectively), especially if compared with cationic clays (0.8 - 1.5 meq/g).[9] Moreover, these solids display the following characteristic: absence of toxicity, high insolubility, minimal environmental impact and reduced risk of migration within the stone. Being highly versatile, LDH have found widespread applications in many fields, particularly in pharmaceutical,[10] heterogeneous catalysis,[11] photochemistry[12] and polymer reinforcement.[13] LDH are represented by the general formula: $[M(II)_{1-x}M(III)_x(OH)_2]A_{x/n}\cdot mH_2O$, where M(II) cation is generally Mg, Zn, Ni, Co or Cu and M(III) cation is Al, Cr, Fe or Ga. *A* is an exchangeable anion of ionic valence n. The *x* value ranges between 0.2 and 0.4 and determines the ion exchange capacity of the material.[14] Interestingly, the well known selectivity scale, $CO_3^{2-} > SO_4^{2-} >> OH^- > F^- > Cl^- > Br^- > NO_3^- > ClO_4^-$, shows the high affinity of LDH towards sulphate anions and makes this material a good candidate to capture the sulphates from gypsum.[15] Layered zirconium phosphate $\alpha\text{-}Zr(HPO_4)_2\cdot H_2O$, is a multipurpose material employed as ion exchanger,[16] polymer filler,[17] catalyst,[18] drug delivery system and many others.[19] Each layer consists of a plane of zirconium atoms bridged by phosphate groups situated above and below the plane. Adjacent layers display a d-spacing of 7.6 Å and create zeolitic cavities containing water molecules.[14] The protons facing inside of the interlayer region can be substituted with alkali metals, obtaining full or half exchanged form.

Finally, both the inorganic solids are used as adsorbent of inorganic and organic pollutant[20] and, besides the gypsum removal, they could intercalate the pollutants absorbed on the gypsum layer grown on the carbonate stones.

In the present work the anion exchange properties of LDH coupled with the cation exchange properties of ZrP were exploited to realize a new cleaning system for the removal of 'black crusts'. Specifically, sub-micrometric chloride form of MgAl LDH (MgAlCl) and the semisodic form of microcrystalline α-zirconium phosphate (ZrPNaH) were employed.

The aim is to combine the two ion exchangers to capture both the calcium and sulphate ions of gypsum, thus promoting the dissolution of the 'black crust' through short contact times. In the first part of the work we investigated the ability of MgAlCl to intercalate sulphate anion directly from

View Article Online
DOI: 10.1039/C7DT03957C

gypsum in powder, via Cl^-/SO_4^{2-} anion exchange reaction. At the same time, we studied the capture of the calcium cations from gypsum in powder by ZrPNaH via Na^+ and H^+/Ca^{2+} cation exchange. Finally, the combined effect of the two ion exchangers on the gypsum dissolution was assayed both towards the gypsum powder and towards a gypsum crust grown on a stone. The cleaning system was studied by X-Ray powder diffraction (XRD) analysis, FE-SEM and EDX analysis.

Experimental

Materials

$CaSO_4 \cdot 2H_2O$, $Na_2SO_4 \cdot 10H_2O$, NaCl, $CaCl_2$, ethylene glycol are *C. Erba RP ACS* products. All other reagents were supplied by *Sigma-Aldrich Chemicals*. The sandstone sample was collected from an ancient side wall in Perugia.

Synthesis of MgAlCl

The LDH with formula $[Mg_{0.65}Al_{0.35}(OH)_2]Cl_{0.35} \cdot 0.6H_2O$ (hereafter MgAlCl), FW= 82.5 and IEC=4.25 meq/g, was synthesised using the modified urea method.[21] A volume of 250 mL of 1 M solution of Mg(II) and Al(III), having molar fraction, x = Al(III)/(Mg(II) + Al(III)), of 0.30, was prepared by dissolving 35.6 g (175 mmol) of $MgCl_2 \cdot 6H_2O$ and 18.1 g (75 mmol) of $AlCl_3 \cdot 6H_2O$ in a water/ethylene glycol 1:4 (v/v) mixture. A total of 27 g (450 mmol) of urea was then added to this solution so that the urea/Al molar ratio was 6. The clear solution was then kept under reflux and under constant stirring for 4 hours. The solid material obtained was recovered by centrifugation and washed two times with deionized water. The product was kept in the wet state in order to favour both the ion diffusion during the ion exchange reactions and the adhesion of the sticky mass to the stone. The weight percent of dried solid in the wet paste, determined by drying in oven at 80°C, was 24 wt%.

Preparation of $MgAlSO_4$

The sulphate form of LDH, with formula $[Mg_{0.65}Al_{0.35}(OH)_2](SO_4)_{0.175} \cdot 0.6H_2O$ (hereafter $MgAlSO_4$) (FW: 86.7 g/mol), was obtained from MgAlCl via anion-exchange process; in particular, 1 g of dry MgAlCl was dispersed in 42 mL of a 0.1M Na_2SO_4 solution (Cl^-/SO_4^{2-} molar ratio 1:1) prepared using CO_2-free deionized water. The dispersion was left under stirring for 3 hours, then centrifugated and washed three times. The obtained wet paste was characterized by 24 wt% of solid content.

Preparation of crystalline α-ZrP

Crystalline zirconium phosphate was prepared by the direct precipitation method in the presence of hydrofluoric acid.[22]

View Article Online
DOI: 10.1039/C7DT03957C

Synthesis of ZrPNaH

The semisodic form of zirconium phosphate (hereafter ZrPNaH), FW= 395 and IEC=5.06 meq/g, was obtained from a colloidal dispersion of microcrystalline zirconium phosphate, obtained by titrating a suspension of 2 g of microcrystalline zirconium phosphate in 100 ml of water with 66.4 ml of 0.1 M propylamine. The dispersion was kept under stirring for 24 hours, then 42 ml of this solution were transferred in a beaker and heated up to 80°C. Once the temperature was reached, 85 ml of a 0.1 M NaCl solution was added to the dispersion and the mixture was left under stirring at 80 °C for 1 hour. The solid was separated from the solution by centrifugation and washed two times with deionised water. A gelatinous precipitate was obtained containing 4 wt% dried product and having formula $Zr(NaPO_4)(HPO_4)\cdot 5H_2O$.

Uptake of sulphate and calcium of gypsum by MgAlCl and ZrPNaH

A weighted amount of MgAlCl or ZrPNaH, in the form of wet paste, was gently mixed with an amount of gypsum so that the Cl^-/SO_4^{2-} or $(Na^+ + H^+)/Ca^{2+}$ equivalent ratio was 2:1, system T1 and T2 of Table 1. The mixtures were analyzed by XRD over time.

The same mixture was prepared mixing the wet paste of MgAlCl and of ZrPNaH with gypsum, system T3 of Table 1.

Table 1 Amount of gypsum, MgAlCl and ZrPNaH as wet paste used to study the sulphate and calcium uptake

	T1		*T2*		*T3*		
	MgAlCl	*Gypsum*	*ZrPNaH*	*Gypsum*	*MgAlCl*	*ZrPNaH*	*Gypsum*
mg	*833 (200)**	*36*	*2500 (100)**	*22*	*417 (100)**	*2500 (100)**	*22*
meq	*0.85*	*0.42*	*0.51*	*0.26*	*0.42*	*0.51*	*0.26*

* Corresponding amount of dry MgAlCl and ZrPNaH

Characterization

The cation content of both MgAlCl and ZrPNaH was determined by Inductively Coupled Plasma Optical Emission Spectrometer (ICP-OES) Varian 700-ES Series after dissolving the samples in concentrated HNO_3 and properly diluting them. The structural characterization was performed by a *PHILIPS X'PERT APD* diffractometer operating at 40 kV and 40 mA, step size 0.05 2θ degree, step scan 30 s, equipped with a *X'Celerator* detector, using the Cu Kα (λ=1.54 Å) radiation.

The morphology of the samples was investigated a FEG LEO 1525 scanning electron microscope (FE-SEM). FE-SEM micrographs were collected after depositing the samples on a stub and coating with a layer of chromium of 8-10 nm.

View Article Online
DOI: 10.1039/C7DT03957C

The elemental mapping of samples was conducted by using energy dispersive X-ray spectroscopy (EDX) supported by a field emission scanning electron microscope (FE-SEM) (FEG LEO 1525).

Results and Discussion

Reaction of MgAlCl with gypsum

In the presence of water, $[Mg_{0.65}Al_{0.35}(OH)_2]Cl_{0.35}\cdot 0.6H_2O$, hereafter MgAlCl, is expected to exchange the chloride counter-ion with the sulphate anions in equilibrium with gypsum, thus leading to the formation of the $MgAlSO_4$ phase according to the following reactions:

$CaSO_{4(s)} \leftrightarrows Ca^{2+}_{(aq)} + SO_4^{2-}{}_{(aq)}$ (1)

$MgAlCl_{(s)} + 1/2\ SO_4^{2-}{}_{(aq)} \leftrightarrows MgAl(SO_4)_{0.5(s)} + Cl^-_{(aq)}$ (2)

Figure 1 shows the XRD patterns of the MgAlCl and $MgAlSO_4$ phases, synthesized as reported in the experimental sections, and that of crystalline gypsum powder. The MgAlCl phase (Figure 1(a)) exhibits a first reflection at 11.42° 2θ, associated to the *(003)* crystallographic planes and corresponding to an interlayer distance of 7.74 Å. The first reflection of the wet $MgAlSO_4$ phase (Figure 1 (b)) is at 8.07° 2θ and corresponds to an interlayer distance of 10.95 Å; in the dry phase of $MgAlSO_4$ the first peak is shifted to 10.0° 2θ (8.84 Å).[23] These data show that the MgAlCl and $MgAlSO_4$ phases are clearly distinguishable by considering the position of the first peaks in the corresponding diffraction patterns; in this way the formation of a significant amount of $MgAlSO_4$, by reaction of MgAlCl with calcium sulphate, can be easily detected by XRD analysis.

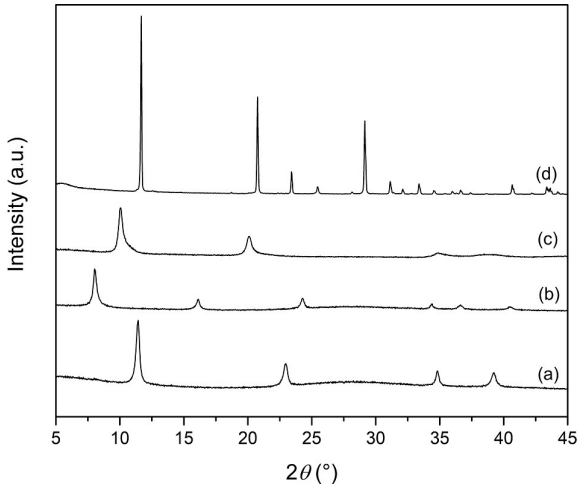

Fig. 1 XRD patterns of MgAlCl (a); wet $MgAlSO_4$ (b); dry $MgAlSO_4$ (c); gypsum (d).

In order to test the reactivity between MgAlCl and gypsum (Gy), a weighted amount of the wet paste of MgAlCl was mixed with a suitable amount of $CaSO_4$ powder, so that the Cl^-/SO_4^{2-} equivalent ratio was 2:1 (T1 system, see Table 1 in experimental section).

View Article Online
DOI: 10.1039/C7DT03957C

The XRD pattern of T1, collected immediately after the addition of gypsum (the time passed between the gypsum addition and the end of the XRD measure was 10 min), is shown in Figure 2. The peaks of the wet $MgAlSO_4$ phase are observed besides those of MgAlCl, indicating that the Cl^-/SO_4^{2-} ion exchange takes place, even though, it is not completely successful as proved by the presence of the reflections of the unreacted gypsum that are mostly overlapping those of MgAlCl phase. The higher charge of sulphate in comparison with chloride anions generates stronger Coulombic attraction with the metal hydroxide layer and determines the higher affinity of sulphate ions toward LDH.[15] After a first bursting step, the reaction does not proceed with time: the pattern of the mixture, stored in a desiccator with 95% of relative humidity (R.H.) and registered few hours later, shows no further reaction advancement (data not shown).

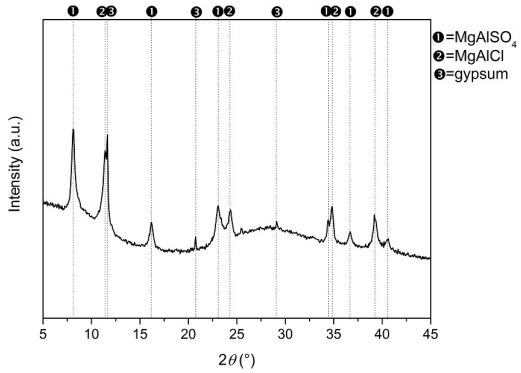

Fig. 2 XRD pattern of the T1 wet mixture.

It is also interesting to observe that the XRD patterns of T1 significantly changes during dehydration, as shown in Figure 3. Specifically, the intensity of the peaks associated with $MgAlSO_4$ decreases while those of MgAlCl and gypsum progressively increase, suggesting that both the backward reactions (1) and (2) are favoured as a consequence of the dehydration.

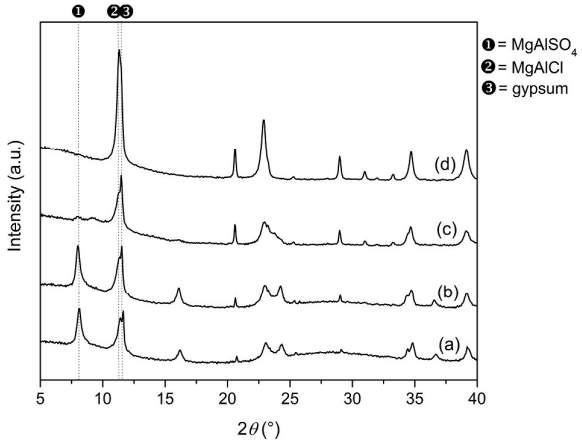

View Article Online
DOI: 10.1039/C7DT03957C

Fig. 3 XRD spectra of T1 at different hydration degree: wet mixture (a); after 2 h of air exposition (b); after 4 h of air exposition (c); dry T1 mixture (d).

Two main distinct reasons can be adduced to explain this phenomenon:

(a) the reaction (2) moves towards the reverse direction: this is due to the increase of the free chloride ions concentration in the mixture, as a result of water evaporation, which acts as driving force for the release of sulphate ions from the interlayer region of LDH to the liquid phase of the paste;

(b) the reaction (1) moves towards the reverse direction: this is due to the presence of free calcium ions that facilitates the replacement of SO_4^{2-} with Cl^- in the LDH interlayer space by removing SO_4^{2-} from the aqueous phase through the precipitation of $CaSO_4$, a poorly water-soluble salt.

The reaction of $MgAlSO_4$ with NaCl and $CaCl_2$ (powder) was investigated to highlight the chloride and calcium ions role (see supporting information).

These findings also show that in the mixture T1 the gypsum undergoes a dissolution and re-precipitation process that, very likely, leads a different type of gypsum (secondary gypsum) in terms of morphology and size of crystals. Indeed, a large number of publications concerns the effect of organic and/or inorganic species on the nucleation, growth kinetics, and morphology of gypsum crystals and on the crystal growth inhibition.[24] Although, an accurate study on the effect of LDH on the gypsum precipitation was not the aim of this work, it was of interest to investigate if the morphology of the secondary gypsum was different from that of primary gypsum. To this end, the pattern of the dried paste T1 was compared with that obtained by mixing the two powdered samples in the same weight ratio as that of the dried paste (Figure 4). The dried paste T1 shows two major differences with respect to the physical mixture: a) the ratio between the intensity of reflections of LDH and gypsum is higher; (b) the reflections of gypsum are broadened. The difference a) should be due to a lower amount of crystalline gypsum re-precipitated and the difference b) to a smaller crystalline domain size of the secondary gypsum with respect to the primary gypsum.

These facts also suggest that the secondary gypsum, eventually re-precipitated on a treated surface of a monument as a consequence of the paste drying, probably exhibits a different adherence from that constituting the original crust and should be removed more easily by the use of a brush.

View Article Online
DOI: 10.1039/C7DT03957C

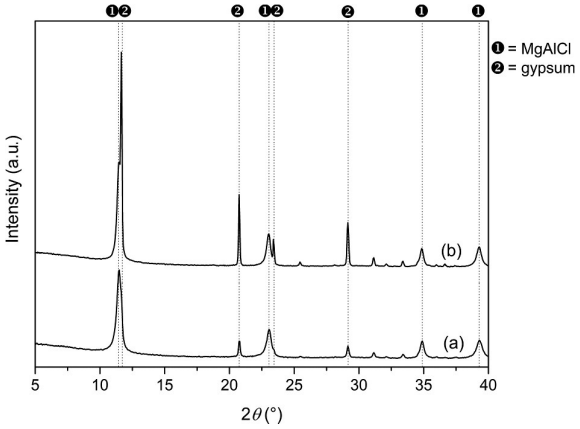

Fig. 4 XRD patterns of dry T1 (a); MgAlCl/gypsum physical mixture (b).

Reaction of ZrPNaH with gypsum

In order to avoid or, at least, limit the re-precipitation of gypsum, as a consequence of the reaction between $MgAlSO_4$ and Cl^- in the presence of free calcium ions, two ways can be followed: the first one consists in keeping the mixture humid by covering it with a plastic film during the application. This approach has a limit: the paste could not be easily removed if it is not completely dried, especially if the surface of the substrate is not smooth. The second way involves the introduction of a solid cation exchanger that is able to capture free calcium ions, preventing or hindering them to precipitate as gypsum.

The cation exchanger selected for this purpose is half sodium exchanged α-zirconium phosphate, $Zr(NaPO_4)(HPO_4)\cdot 5H_2O$, hereafter ZrPNaH, prepared in a gel form as reported in the experimental section. The XRD pattern of the gelatinous sample is shown in Figure 5. Two reflections are clearly visible: the first one at 7.44° 2θ, corresponding to an interlayer distance of 11.8 Å, and one reflection at 33.8° 2θ, characteristic of the *(020)* crystallographic planes of the α-type phase. The ion exchange properties of ZrPNaH were initially tested separately from MgAlCl, adding gypsum to the ZrPNaH gel so that the $(Na^+ + H^+)/Ca^{2+}$ equivalent ratio was 2, mixture T2 of Table 1. After putting in contact ZrPNaH with gypsum the XRD pattern changes (Figure 6). In particular, besides the reflections typical of gypsum, the pattern of wet T2, collected immediately after the contact, shows a decrease of the peak intensity at 7.44° 2θ and the appearance of a new reflection around 8.8° 2θ, corresponding to an interlayer distance of 10 Å, typical of the half-exchanged α- zirconium calcium phosphate phase ($Zr(Ca_{0.5}PO_4)(HPO_4)\cdot 3H_2O$, hereafter ZrPCaH).[25] The patterns collected on the wet system over time show a first order phase transition from the ZrPNaH phase to the ZrPCaH phase. In particular, after 24 hours from the beginning of the experiment, T2 is mainly constituted of the ZrPCaH phase and only a little amount of ZrPNaH and of gypsum crystalline phase are still present (Figure 6 (d)). Upon the dehydration, the gypsum reflection increases very

View Article Online
DOI: 10.1039/C7DT03957C

likely due to a partial calcium release from ZrPCaH promoted by the increase of the free sodium and sulphate ions concentration, as previously observed and discussed in the T1 system. The above experiment suggests that the ZrPNaH gel is able to subtract calcium ions from gypsum through an ion exchange reaction, so that it results to be suitable to be mixed with MgAlCl, in order to make the dissolution of gypsum more efficient. Moreover, the synergic action of the two exchangers could hinder the gypsum re-precipitation during the dehydration process.

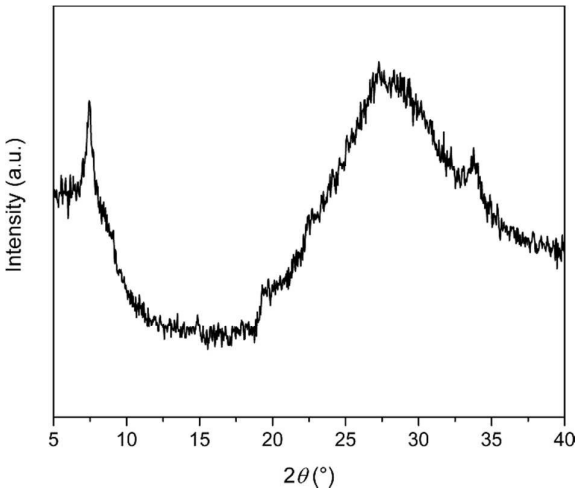

Fig. 5 XRD spectrum of hydrated ZrPNaH.

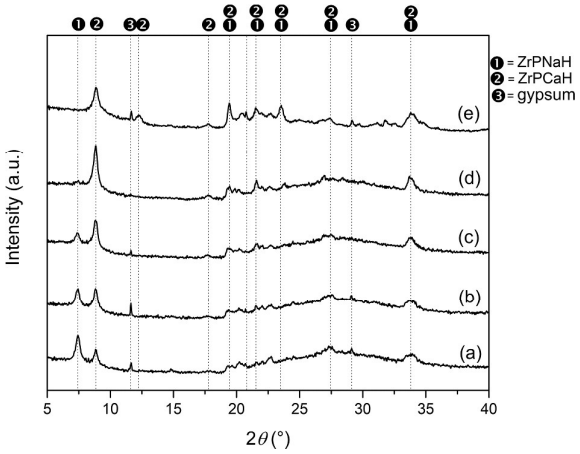

Fig. 6 XRD spectra of wet T2 at different reaction times: as prepared (a); 15 min (b); 1 h (c); 24 h (d); dry (e).

Combined action of MgAlCl and ZrPNaH

The efficiency of the MgAlCl/ZrPNaH system on the gypsum dissolution was tested on a 1:1 (w/w) mixture. Figure 7 (a) shows the XRD pattern of the MgAlCl/ZrPNaH wet paste before mixing with gypsum: the typical reflections of both MgAlCl and ZrPNaH phases are observed. In Figure 7, the XRD patterns of the MgAlCl/ZrPNaH system mixed with powdered gypsum (hereafter T3, Table 1) are also reported: pattern (b) refers to the system kept in a desiccator for 24 hours under 95 % R.H.,

View Article Online
DOI: 10.1039/C7DT03957C

while pattern (c) refers to same system dried in an oven at 35°C. With respect to MgAlCl/ZrPNaH wet paste, the XRD pattern of T3 wet paste shows:

- the disappearance of the MgAlCl phase and the appearance of the $MgAlSO_4$ phase;
- the disappearance of the ZrPNaH phase and the appearance of the ZrPCaH phase;
- the absence of the gypsum crystalline phase.

All these results suggest that the MgAlCl/ZrPNaH wet paste is able to quickly dissolve gypsum through ion exchange reactions involving both MgAlCl and ZrPNaH according to the reaction:

$$MgAlCl + ZrPNaH + ½\ CaSO_4 \leftrightarrows MgAl(SO_4)_{0.5} + ZrPCa_{0.5}H + NaCl \quad (3)$$

Moreover, the efficiency of MgAlCl/ZrPNaH in the gypsum dissolution is increased in comparison with T1 and T2 systems as proved by the disappearance of MgAlCl, ZrPNaH and gypsum phases.

In this regard it should be observed that the complete solubilization of $CaSO_4$ according to reaction (3) does not imply necessarily the disappearance of MgAlCl since the experiment was carried out with an excess of LDH with respect to gypsum. Therefore, the absence of the MgAlCl reflections seems to indicate that the residual chloride ions are solubilized in the sulphate phase, thus forming a solid solution with the interlayer distance of pure $MgAlSO_4$. The formation of solid solutions in LDH containing two different anions, with comparable dimensions, is known[26] and, in the present work, is supported by the data reported in the supporting information. After drying, the pattern of T3 mixture further changes. Specifically, similarly to T1, the drying process promotes the regeneration of MgAlCl crystalline phase from the $MgAlSO_4$; however, differently form T1, the presence of NaCl phase indicates that this process took place only partially. Once again, the absence of the $MgAlSO_4$ reflections seems to indicate that the residual sulphate ions are solubilised in chloride phase (see supporting information). Moreover, the presence of a significant amount of ZrPCaH and the lack of gypsum reflections proves that the majority of gypsum has been successfully dissolved.

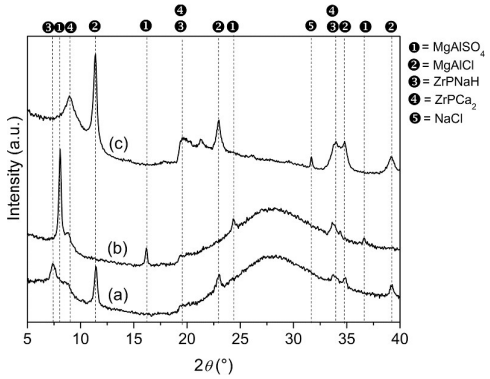

Fig. 7 XRD patterns of: pristine MgAlCl/ZrPNaH wet paste (a); T3 mixture equilibrated for 24 hours at 95% R.H. (b); after drying in an oven at 35°C (c).

View Article Online
DOI: 10.1039/C7DT03957C

In order to rule out the possibility to damage the stone underneath the crust, the paste was mixed with both gypsum and $CaCO_3$ and the XRD spectrum of the mixture (see in supporting information) proves that the paste is not harmful toward the marbles or other calcium carbonate based stones.

A comparative observation of the SEM image and of the EDX element mappings of the MgAlCl/ZrPNaH/Gy physical mixture and of the T3 dried paste enables to verify the morphology of the materials before and after the ionic exchange reactions. Figure 8 (a) and (b) show the SEM images of the MgAlCl/ZrPNaH physical mixture at two different magnifications. The EDX image of Figure 8 (b) allows to correctly assign the particles to the different solids by the distribution of Mg and Zr that identifies the LDH and ZrP particles, respectively. The ZrPNaH is arranged in big aggregates of dimensions ranging from 10 to 50 μm. The MgAlCl is constituted by well grown hexagonal platelets with a diameter of about 750 nm, which are attached all over the ZrP surface. Figure 8 (d)-(f) show the SEM and EDX of MgAlCl/ZrPNaH/Gy physical mixture, where the needle-type crystals of gypsum, identifiable by the Ca mapping, are well evident beside the LDH and ZrP particles. Note that part of the LDH platelets are distributed over the gypsum crystals, indicating an affinity of the LDH for the gypsum surfaces.

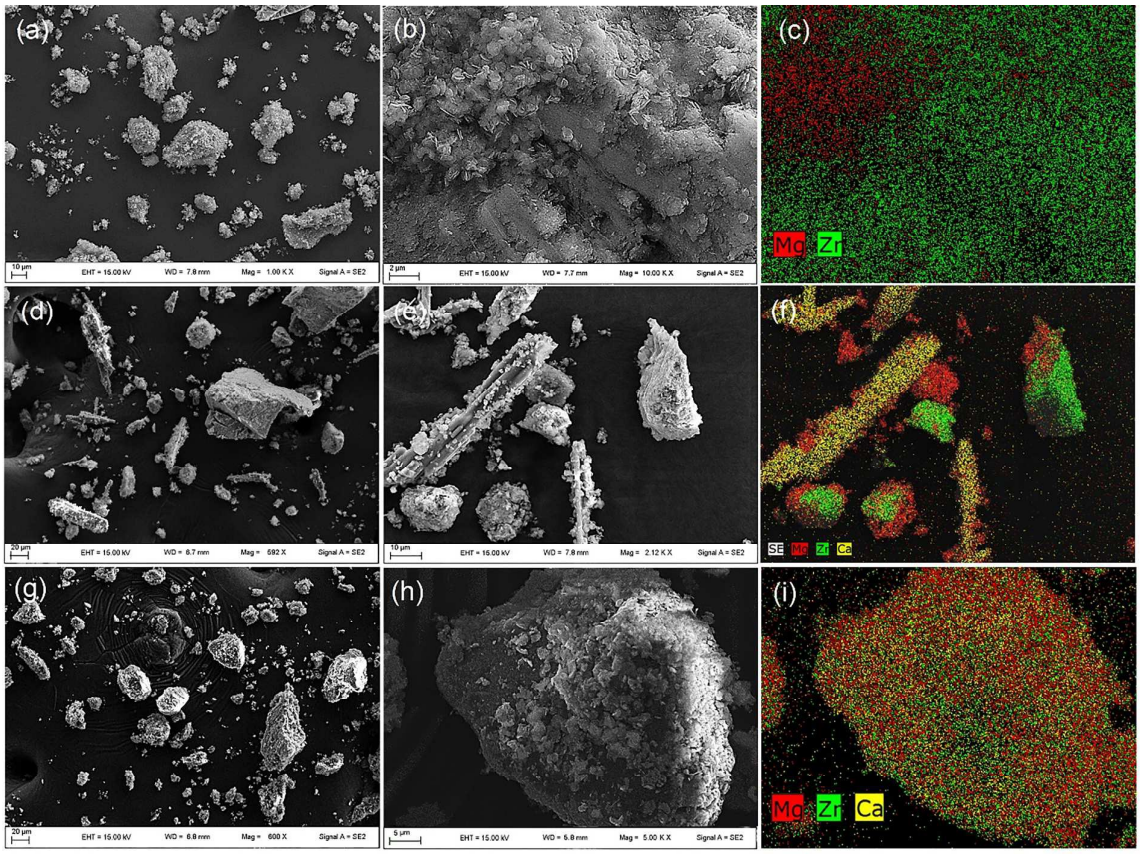

Fig. 8. SEM and EDX element mappings of the MgAlCl/ZrPNaH physical mixture (a-c); MgAlCl/ZrPNaH/Gy physical mixture (d-f); dry T3 (g-i).

View Article Online
DOI: 10.1039/C7DT03957C

In the dry T3 mixture, where gypsum was mixed together with the wet paste and then dried, only aggregates of ZrP and LDH are visible (Figure 8 (g) and (h)); however, the EDX analysis (Figure 8 (i)) shows a uniform distribution, throughout the sample under examination, of Mg, Zr and Ca ions, suggesting an intimate interaction among the components. Moreover, the absence of large gypsum crystals confirms the role of LDH and ZrP in the gypsum dissolution, as assessed by XRD.

Application of the MgAlCl/ZrPNaH paste on sandstone black crust

A sample of black crust grown on a fragment of sandstone was collected from a historical wall of the University of Perugia. Sandstone is a sedimentary rock, composed by calcite, feldspars and iron oxides, particularly diffused in the buildings of central Italy. Similarly to marble, the presence of calcite allows the formation of a black crust layer on its surface.[27] A picture of the selected sample, before treatment, is shown in Figure 9 (a). As proved by XRD, the main components of the crust are gypsum, quartz and calcite (Figure 10, pattern (a)). The wet paste, consisting of MgAlCl/ZrPNaH 1:1 (w/w), was spread on a 3 x 4.5 cm sample area (Figure 9 (b)): the paste was left for 75 min and removed before it became completely dry (Figure 9 (c)) to avoid the possible deposition of recrystallized gypsum over the substrate. A second 75 min treatment was carried out on the same area. After each treatment a thin layer of crust was stucked to the removed paste, uncovering an irregular, rough and grainy surface, much clearer than the initial one (Figure 9 (d)).

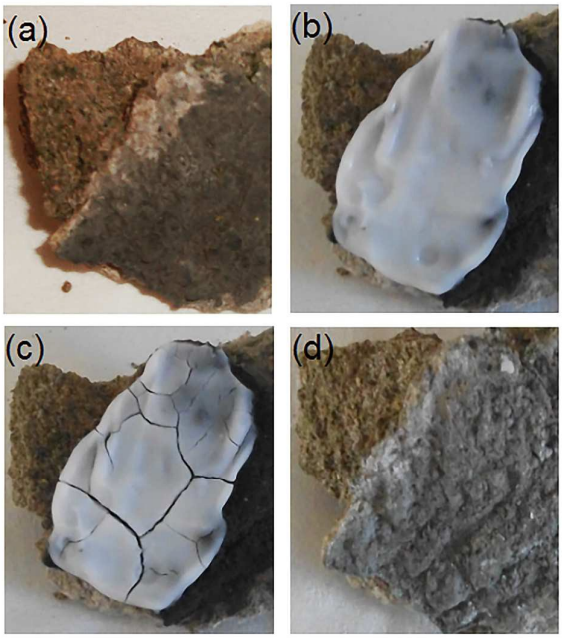

Fig. 9 Phases of application of the MgAlCl/ZrPNaH paste on the sandstone black crust: untreated sample (a); wet paste just after the first application (b); wet paste just before being removed (c); sample after two treatments (d).

View Article Online
DOI: 10.1039/C7DT03957C

The XRD pattern of the poultice removed after the first treatment, before the complete dehydration (pattern (b) of Figure 10), is rather complicated, due to the presence of several components. However, the following observation can be pointed out:

- the wet paste contains both quartz and calcite;
- the typical peaks of crystalline gypsum are missing, while the peaks due to the $MgAlSO_4$ crystalline phase are clearly distinguishable, thus indicating the solubilisation of gypsum;
- weak and broad peaks due to MgAlCl and ZrPCa(Na)H crystalline phases are observed.

The XRD (Figure 10 (c)) collected after the drying process of the removed paste resulted in a few modications. The main changes regard the reconvertion of $MgAlSO_4$ in MgAlCl and the appearance of NaCl. A remarkable aspect is the absence of the gypsum and of crystalline ZrPCaH phase. The latter issue can be justified considering that the ZrPCaH reflections are hidden whitin the pattern background.

The above results are in agreement with those previously obtained for the reaction of the MgAlCl/ZrPNaH system with gypsum powder, and confirm the ability of the mixture of the two ion exchangers to dissolve gypsum even in the form of consolidated crust, or, possibly, to reprecipitate it in an a less compact and amorphous layer, which can be more easily removed. The change of colour of the sandstone rock, after having removed the wet paste and washed the stone surface, further supports the effectiveness of the treatment.

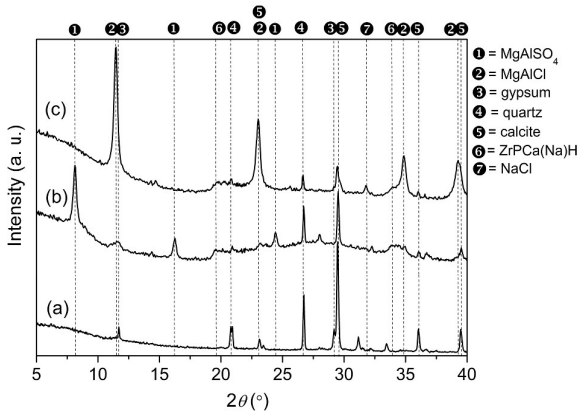

Fig. 10 XRD patterns of: sandstone black crust before treatment (a); hydrated MgAlCl/ZrPNaH (b) and dry MgAlCl/ZrPNaH (c) applied over the sandstone black crust after 75 min.

SEM and EDX analysis were perfomed on the sandstone black crust and on the dry MgAlCl/ZrPNaH recovered after the first treatment on the black crust. The SEM image in Figure 11 (a) shows a particle of 32 x 17 μm, surrounded by brighter and irregular grains with Ca and S as main components. The elemental distribution maps of the first particle (Fig. 11 (b)-(d)) revealed an high amount of Si related to quartz, which is consistent with the X-ray diffraction analysis, while

View Article Online
DOI: 10.1039/C7DT03957C

the little amount of Ca and S, is attributed to gypsum. However, the calcium and sulphur mapping are not exactly overlapping due to the contribution of calcite to the Ca mapping (Figure 11 (b) and (c)). The SEM image of the dry paste collected after the treatment (Figure 11(e)) shows the presence of big aggregates where the single particles are not distinguishable. Information about the composition of these aggregates was obtained by means EDX elemental mapping of Zr, Mg, S, Ca and Si (Figure 11 (f)-(k)). The aggregates are mainly composed of ZrP and LDH (very bright spots for Zr and Mg) and the sulphur appears homogeneously distributed whithin the sample, proving the incorporation of gypsum in the dry paste similarly to T3 system. Calcium mapping reveals an uniform distributions as the sulphur except for some bright areas that have not correspondence with S, Zr and Mg mapping and that can be ascribable to the calcite. Finally, Si mapping (Figure 11(h)) allows to recognize a quartz particle incorporated in the dry paste. The presence of calcite and quartz particles confirm that a part of the crust was stucked to the paste removed as has been also inferred by the XRD.

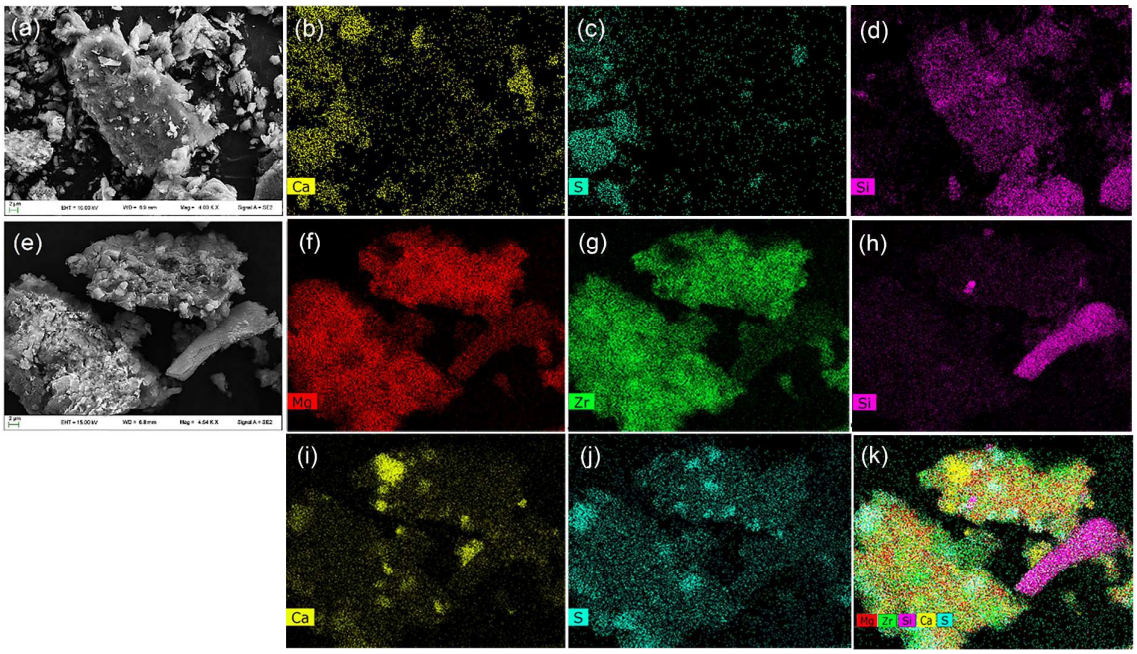

Fig. 11 SEM and EDX element mappings of the sandstone black crust (a-d); dry MgAlCl/ZrPNaH after the first treatment on the black crust (e-k).

Conclusions

This study has demonstrated that LDH reacts easily with gypsum through the Cl^-/SO_4^{2-} exchange reaction helping in the dissolution of the gypsum matrix that composes the black crusts. The synthesis of LDH in form of a paste facilitates its manipulation and application over the surface; moreover, the use of ZrP too favours the reaction by capturing calcium ions without releasing all of

View Article Online
DOI: 10.1039/C7DT03957C

them, even when the paste results completely dry. The presence of ZrP in combination with LDH is also helpful not only to increase the gypsum dissolution, but also to hinder the release of sulphate ions from LDH upon drying, preventing, as far as possible, the formation of secondary gypsum. The joint action of the two ion exchangers produces indeed an even more efficient reaction where calcium and sulphate are successfully substituted by sodium and chloride ions; furthermore, NaCl and the eventual secondary gypsum derived from the backward reaction do not constitute a problem of undesired salt deposition because they remain entrapped within the paste. Moreover, the evidence of a selectivity of the LDH/ZrPNaH paste towards gypsum rather than calcite makes this system safe as regards the stone not damaged by the black crusts. The application of the paste over the sandstone fragment confirms the ability of the mixture of the two ion exchangers to dissolve gypsum even in the form of consolidated crust, or, possibly, to reprecipitate it in an amorphous layer that can be removed more easily. The technique proposed in this study displays both advantages and drawbacks. One of the most important aspects of this method consists in the rapidity of the reaction: compared to other procedures, where the treatments require hours or even days to be effective, in this case, the application lasts a period of time ranging from a few minutes to a few hours, depending on the temperature and on the external humidity. Another factor that should be highlighted is the absence of toxicity and the low cost of the materials employed. Concerning the weak points of the system, the thickness of the layer treated is a relevant aspect to take into consideration: so far, this method seems to be efficient for very thin black crusts, indicating that further tests are necessary to produce a system that can be suitable to remove crusts that are more consistent, avoiding multiple applications. Preliminary studies are now undergoing to employ LDH and ZrP, together with polymers, to remove salt encrustations from the surface of work of arts painted in *affresco* technique. The results of these treatments will be investigated in more detail in another work; however, the present achievements show that layered double hydroxides and zirconium phosphate have once again proved themselves to be multipurpose materials as they can also be successfully applied in the field of art.

Conflicts of interest

There are no conflicts of interest to declare.

Aknowledgements

The authors thank Dr. Alessandro di Michele of the LUNA Laboratory at the Department of Physics and Geology of Perugia University for his valuable contribution to FE-SEM analyses.

View Article Online
DOI: 10.1039/C7DT03957C

Notes and references

1 A. Moropoulou, K. Bisbikou, R. Van Grieken, F. Zezza and F. Macri, *Atmos. Environ*., 1998, **32**, 967–982.

2 L. Lazzarini and M. Laurenzi Tabasso, Il Restauro della Pietra, UTET Scienze Tecniche, Torino, 2010.

3 G. Amoroso and M. Camaiti, Trattato di scienza della conservazione dei monumenti: etica della conservazione, degrado dei monumenti, interventi conservativi, consolidanti e protettivi, Firenze, 2002.

4 P R. Hill and J C E. David, *Practical Stone Masonry*. Donhead, London, 1995.

5 C. Rodríguez-Navarro, K. Elert, E. Sebastián, R.M. Esbert, C.M. Grossi, A. Rojo, F.J. Alonso, M. Montot and J. Ordaz, *Rev. Conserv*. 2003, **4**, 65-82.

6 Exterior Cleaning of Historic Masonry Buildings. Draft. Washington, D.C.: Office of Archeology and Historic Preservation, Heritage Conservation and Recreation Service, U.S. Department of the Interior, 1976.

7 F. Cappitelli, E. Zanardini, G. Ranalli, E. Mello, D. Daffonchio and C. Sorlini, *Appl. Environ. Microbiol*., 2006, **72**, 3733–3737.

8 N. Ashurst, Cleaning Historic Buildings, volume 2, Donhead Publishing, 1994.

9 (a) B.K.G. Theng, "*The Chemistry of Clay-Organic Reactions*", Adam Hilger, London (1974); (b) F. Bergaya, B.K.G. Teng and G. Lagaly Eds., "*Handbook of Clay Science*", Elsevier (2006).

10 (a) *Clays and Health Clays* in *Pharmacy, Cosmetics, Pelotherapy, and Environmental Protection,* Special Issue of *Appl. Clay Sci.* ed. M I. Carretero and G. Lagaly, 2007, **36**; (b) V. Ambrogi, V. Ciarnelli, M. Nocchetti, L. Perioli and C. Rossi, *Eur. J. Pharm. Sci.*, 2009, **73**, 285–291; (c) *LDH in physical, chemical, bio-chemical and life sciences* in *Developments in Clay Science* – Volume 5B Handbook of Clay Science: Techniques and Applications, ed. F. Bergaya and G. Lagaly, 2013, vol. 5B; (d) V. Rives, M. del Arco and C. Martín, *Appl. Clay Sci.*, 2014, **88-89**, 239-269; (e) S. Saha, S. Ray, R. Acharya, T. K. Chatterjee and J. Chakraborty, *App. Clay Sci.*, 2017, **135**, 493–509.

11 (a) A. Vaccari, *Appl. Clay Sci.*, 1999, **14**, 161-168; (b) T. Montanari, M. Sisani, M. Nocchetti, R. Vivani, M. Concepcion Herrera Delgado, G. Ramis, G. Busca and U. Costantino, *Catal. Today,* 2010, **152**, 104-109; (c) A. Fronzo, C. Pirola, A. Comazzi, C. L. Bianchi, A. Di Michele, R. Vivani, M. Nocchetti, M. Bastianini, D. C. Boffito and F. Galli, *Fuel*, 2014, **119**, 62–69; (d) G. Fan, F. Li, D. G. Evans and X. Duan, *Chem. Soc. Rev.*, 2014, **43**, 7040-7066; (e) L. Fagiolari, A. Scafuri, F. Costantino, R. Vivani, M. Nocchetti and A. Macchioni, *ChemPlusChem*, 2016, **81**, 1060-1063. (f) K. Mori, T. Taga and H. Yamashita, *ACS Catal.,* 2017, **7**, 3147−3151.

View Article Online
DOI: 10.1039/C7DT03957C

12 L. Mohapatra and K. Parida, *J. Mater. Chem. A*, 2016, **4**, 10744–10766.

13 (a) U. Costantino, F. Costantino, F. Elisei, L. Latterini and M. Nocchetti, *Phys.Chem. Chem. Phys.,* 2013, **15**, 13254-13269. (b) D. G. Evans and X. Duan, *Chem. Commun.*, 2006, 485-496; (c) J. Yu, Q. Wang, D. O'Hare and L. Sun, *Chem.Soc.Rev.*, DOI: 10.1039/c7cs00318h.

14 Rives, V. In Layered Double Hydroxides: Present and Future; Rives, V., Ed.; Nova Science Publishers: New York, 2001.

15 (a) S. Miyata, *Clays Clay Miner*., 1983, **31**, 305-311; (b) L. Parker, N. Milestone and R. Newman, *Ind. Eng. Chem. Res.*, 1995, **34**, 1196-1202; (c) S. V. Prasanna and P. Vishnu Kamath, *Ind. Eng. Chem. Res.*, 2009, **48**, 6315–6320; (d) S.H.J. Eiby, D.J. Tobler, S. Nedel, A. Bischoff, B.C. Christiansen, A.S. Hansen, H.G. Kjaergaard and S.L.S. Stipp, *Appl. Clay Sci*., 2016, **132–133**, 650–659.

16 A. Clearfield and U. Costantino, in Comprehensive Supramolecular Chemistry, G. Alberti, T. Bein Eds; 1996, **7**, Ch 4 Pergamon, Elsevier Science Ltd. Press: New York.

17 (a) M. Casciola, D. Capitani, A. Comite, A. Donnadio, V. Frittella, M. Pica, M. Sganappa and A. Varzi, *Fuel Cells*, 2008, **3–4**, 217–224; (b) M. Casciola, G. Alberti, A. Donnadio, M. Pica, F. Marmottini, A. Bottino and P. Piaggio, *J. Mater. Chem*., 2005, **15**, 4262–4267; (c) M. Pica, A. Donnadio and M. Casciola, *Starch/Starke*, 2012, **64**, 237–245; (d) M. Pica, A. Donnadio, D. Capitani, R. Vivani, E. Troni and M. Casciola, *Inorg. Chem*. 2011, **50**, 11623–11630; (e) M. Pica, A. Donnadio, M. Casciola, P. Cojocaru and L. Merlo, *J. Mater. Chem*., 2012, **22**, 24902-24908; (f) R. Bongiovanni, M. Casciola, A. Di Gianni, A. Donnadio and G. Malucelli, *Eur. Polym. J*. 2009, **45**, 2487–2493; (g) L Sun., W. J. Boo, D Sun., A. Clearfield and H. J. Sue, *Chem. Mater.*, 2007, **19**, 1749-1754; (h) W. J. Boo, L. Y. Sun, J. Liu, A. Clearfield, H. J. Sue, M. J. Mullins and H. Pham, *Compos. Sci. Technol.*, 2007, **67**, 262-269; (i) H. J Sue, K. T. Gam, N. Bestaoui, N. Spurr and A. Clearfield, *Chem. Mater.*, 2004, **16**, 242-249; (j) Q, Tai, Y. Kan, L. Chen, W. Xing, Y. Hu and L. Song, *React. Funct. Polym.*, 2010, **70**, 340-345; (k) H. Zhang, L. Chen, X. Han, F. Jiang, H. Sun and D. Sun, *RSC Adv.*, 2017, **7**, 32682-32691.

18 (a) M. Pica, *Catalysts* 2017, **7**, 190; (b) D. Ballesteros-Plata, A. Infantes-Molina, E. Rodríguez-Aguado, P. Braos-García, J. Jiménez-Jiménez and E. Rodríguez-Castellón, *Catalysts*, 2017, **7**, 176; (c) O. Shimomura, K. Tokizane, T. Nishisako, S. Yamaguchi, J. Ichihara, M. Kirino, A. Ohtaka and R. Nomura, *Catalysts*, 2017, **7**, 172; (d) J. Sanchez, M.V. Ramos-Garcés, I. Narkeviciute, J.L.Colón and T.F. Jaramillo, *Catalysts*, 2017, **7**, 132.

19 (a) H. Kalita, B. P. Kumar, S. Konar, S. Tantubay, M. K. Mahto, M. Mandal and A. Pathak. *Mater. Sci. Eng: C*, 2016, **60**, 84-91; (b) V. Saxena, A. Diaz, A. Clearfield, J. D. Batteas and M. D. Hussain, *Nanoscale*, 2013, **5**, 2328-2336; (c) M- L- González, M. Ortíz, C. Hernández, J. Cabán, A.

View Article Online
DOI: 10.1039/C7DT03957C

Rodríguez, J. L. Colón and A. Báez, *J. Nanosc. Nanotechno.*, 2016, **16**, 117-129; (d) J. L. Colón and B. Casañas, 2015, *Tailored Organic-Inorganic Materials*, E. Brunet, J. Colòn, A. Clearfield Eds. Wiley, 395-437; (e) A. Donnadio, V. Ambrogi, D. Pietrella, M. Pica, G. Sorrentino and M. Casciola, *RSC Adv.*, 2016**, 6**, 46249-46257.

20 (a) Q. Zhang, Y. Li, P. Phanlavong, Z. Wang, T.Jiao, H. Qiu and Q. Peng, *J. Clean. Prod.*, 2017, **161**, 317-326; (b) Q. Zhang, Q. Du, T. Jiao, B. Pan, Z. Zhang, Q. Sun, S. Wang, T. Wang and F. Gao, *Chem. Eng. J.*, 2013, **221**, 315–321; (c) N.K. Lazaridis, *Water, Air, Soil Pollut.*, 2003, **146**, 127-139.

21 (a) U. Costantino, F. Marmottini, M. Nocchetti and R. Vivani, *Eur. J. Inorg. Chem*., 1998, **10**, 1439-1446; (b) M. Bastianini, D. Costenaro, C. Bisio, L. Marchese, U. Costantino, R. Vivani and M. Nocchetti, *Inorg. Chem.*, 2012, **51**, 2560−2568.

22 G. Alberti, S. Allulli, U. Costantino and M. A. Massucci, *J. Inorg. Nucl. Chem.*, 1975, **37**, 1779.

23 N. Iyi, K. Fujii, K. Okamoto and T. Sasaki, *Appl. Clay Sci.*, 2007, **35**, 218–227.

24 (a) J. Li, G. Li and Y. Yu, *Mater. Lett.*, 2007, **61**, 872–876; (b) A. E. S. Van Driessche, J. M. Garcia-Ruiz, J. M. Delgado-Lopez and G. Sazaki*, Cryst. Growth Des.*, 2010, **10**, 3909–3916; (c) N.B. Singh and B. Middendorf, *Prog. Cryst. Growth Ch.*, 2007, **53**, 57-77; (d) M. Prisciandaro, A. Lancia and D. Musmarra, *Ind. Eng. Chem. Res.,* 2001**, 40***,* 2335-2339.

25 G. Alberti, R. Bertrami, M. Casciola, U. Costantino and J.P. Gupta, *J. Inorg. Nucl. Chem.,* 1976, **38**, 843–848.

26 U. Costantino, R. Vivani, M. Bastianini, F. Costantino and M. Nocchetti, *Dalton Trans*., 2014, **43**, 11587-11596.

27 Rosignoli, R. *Diagnosi sul degrado dei litotipi arenitici in Giornata di studio: Alterazione delle pietre naturali e artificiali: diagnosi e sistemi di risanamento*. 1994.